Carbohydrate Research, 252 (1994) 183–207
Elsevier Science B.V., Amsterdam

Structural roles of calcium ions and side chains in welan: an X-ray study

Rengaswami Chandrasekaran *, Akella Radha and Eun J. Lee

Whistler Center for Carbohydrate Research, Smith Hall, Purdue University, West Lafayette, Indiana 47907-1160 (USA)

(Received June 9th, 1993; accepted July 12th, 1993)

ABSTRACT

Welan is the first branched polymer in the gellan family of polysaccharides whose three-dimensional structure has been determined by X-ray diffraction analysis of polycrystalline and well oriented fibers of the calcium salt. The molecule exists as a half-staggered, parallel, double-helix, similar to that of gellan. The side chains fold back on the main chain to form hydrogen bonds with the carboxylate groups. This shielding enhances the stability of the double-helix. Three molecules are organized in a trigonal unit cell of dimensions $a = 20.83$ and $c = 28.69$ Å with a lateral separation of 12.0 Å in each pair; this is 2.9 Å larger than in gellan. The double helices are in contact with each other through calcium ions and water molecules via $COO^- \cdots Ca^{2+} \cdots COO^-$ and $COO^- \cdots W \cdots Ca^{2+} \cdots COO^-$ interactions, and through side chain–side chain hydrogen bonds. These structural features enable us not only to explain how the side chains in welan are responsible for the enhanced molecular stabilty relative to gellan, but also to show how essential they are for the associative properties which control the rheology of the polymer.

INTRODUCTION

Welan is a branched polysaccharide produced by *Alcaligenes* ATCC 31555. Its chemical structure was originally shown to consist of a pentasaccharide repeating unit (**1**) by Jansson et al.[1] and later confirmed by O'Neill et al.[2] The main chain consists of a tetrasaccharide repeating unit (ABCD), the same as in gellan[3]. Approximately two-thirds of the side chains (E) are α-L-rhamnopyranosyl and the remainder are α-L-mannopyranosyl units. Approximately 85% of the 3-linked glucosyl residues (A) are substituted with *O*-acetyl groups in the 2-position[4].

* Corresponding author.

SSDI 0008-6215(93)E0255-Y

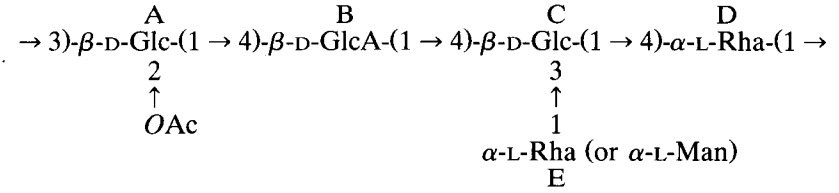

1

Unlike gellan, which forms strong and brittle gels, welan is a nongelling polysaccharide forming highly viscous aqueous solutions which have been shown[5] to be stable up to ~ 130°C. Welan, originally introduced to the oil field in 1985, has unusually good compatibility with calcium and could have potential utility in cementing applications. It may also have utility as an anti-washout additive for underwater concrete placement. In contrast to xanthan and the *Arthobacter* weak gel systems[6–8], welan in water shows no evidence of a conformational transition during heating and cooling between 0 and 100°C. Crescenzi et al.[9] interpreted this in terms of a polymer existing as disordered coils, but there is strong evidence that the normal conformation of welan is a stable ordered structure that resists thermal denaturation in this temperature range[10–13].

An earlier computer modeling study[14], based on X-ray diffraction patterns from noncrystalline fibers of the potassium form, showed that the welan molecule can adopt a gellan-like half-staggered, double-helical conformation[15] in which the side chains fold over the polymer backbone so as to partially shield the carboxylate groups and thus give additional stability to the ordered structure. Further, it was conjectured that the side chains might in some way affect the cation-mediated interactions between double helices and thus be responsible for the weak gelling behavior of welan. The crystal structure of calcium welan obtained from very good fiber diffraction patterns demonstrates that the side chains have dominant structural roles both in the stability of the double helix and in the association of the double helices via cations and water molecules which in turn can be correlated with the unusual physical properties of welan.

EXPERIMENTAL

Fiber preparation.—A sample of clarified welan was provided by Kelco, Division of Merck & Co., San Diego, CA. The polymer was converted into its calcium form by preparing a solution (4 mg/mL) of welan in 100 mM $CaCl_2$ at 90°C with constant stirring. The polysaccharide was first precipitated with two volumes of 2-propanol kept at 0°C. The precipitate was successively rinsed with 80 and 100% 2-propanol in order to remove unbound calcium ions, if any, then washed thoroughly with acetone and vacuum dried. An aqueous solution (2 mg/mL) of this material was mixed well and a small amount placed in the gap between the two glass rods in a fiber puller. The drop was allowed to dry slowly under reduced relative humidity of ~ 75% surrounding the specimen. When the drop reached a

semi-solid state, it was gradually stretched into a fiber (~ 4 mm long and 0.5 mm thick). Fiber density was measured by the flotation method using a mixture of benzene and bromoform.

Diffraction patterns.—Diffraction patterns were recorded on flat photographic films in a pin-hole camera using Ni-filtered Cu$K\alpha$ radiation ($\lambda = 1.5418$ Å). Typical fiber-to-film distance was 35 mm. A steady stream of helium gas, after bubbling through an appropriate saturated salt solution, was used to flush the specimen chamber in order to maintain the fiber at the desired relative humidity and diminish air scattering. Unit cell dimensions were determined by using an internally calibrated pattern obtained from a fiber dusted with calcite powder (of characteristic spacing 3.035 Å).

Intensity measurement.—The diffraction pattern was scanned on an Optronics P-1000 rotating drum microdensitometer with a 100-μm raster step. The pattern was displayed on a Lexidata 3400 raster graphics system interfaced with a VAX 8550 computer. Based on points selected between layer lines, and away from the reflections, the background in the film was estimated and subtracted from the entire pattern. The Bragg intensities were calculated by integrating the optical densities inside each spot boundary. Lorentz and polarization corrections were applied before computing the observed structure amplitudes. The various steps for the intensity measurement are well documented[16–18].

Diffraction data.—Polycrystalline and well oriented fibers of calcium welan, prepared from $CaCl_2$ solutions 25 to 150 mM concentrations, and maintained at 43 to 92% r.h., produced very similar diffraction patterns containing sharp Bragg reflections. The diffraction pattern shown in Fig. 1 is from one of the best

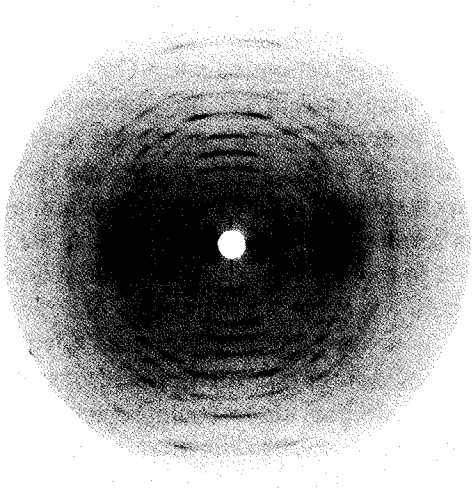

Fig. 1. X-ray diffraction pattern from a well oriented and polycrystalline fiber of calcium welan.

polycrystalline and extremely well oriented fibers corresponding to conditions of 100 mM salt concentration and 75% r.h. The general intensity distribution is of the same kind as observed for K^+ gellan[15] which underlines welan's ability to adopt a gellan-like double helical structure. The spots are well resolved in all the layer lines up to $l = 11$, indicating that the welan specimen is made up of crystallites larger than those in the K^+ gellan specimens.

There are meridional reflections on $l = 3n$ layer lines, and 76 nonmeridional spots are observed up to 2.5 Å resolution. All could be indexed with a trigonal unit cell of dimensions (and estimated standard deviations) $a = b = 20.83(2)$ Å and $c = 28.69(3)$ Å ($V = 10781$ Å^3), which are much larger than the corresponding values $a = b = 15.75$ Å and $c = 28.15$ Å ($V = 6047$ Å^3) for K^+ gellan[15], V being the unit cell volume. A set of 37 "below threshold" spots, which are too weak to be seen on the film, was appended to the list of observed spots in the X-ray data in conducting the structure analysis. The lowest measured intensity of an observed spot was assigned as the threshold value to each weak reflection in this group. Such a reflection was included in the least-squares refinement only when its calculated structure amplitude was higher than the observed amplitude.

Model building and refinement.—A half-staggered, parallel, double helix consisting of two welan chains of three-fold, left-handed helix symmetry, and pitch (P) of 57.4 Å, which is 1.1 Å larger than for K^+ gellan[15], was constructed using the linked-atom least-squares (LALS) method[19]. The details are essentially the same as those reported in the computer modeling of K^+ welan[14].

The major conformational variables in the pentasaccharide unit were the ten glycosidic bridge torsion angles, the eight additional rotations defining the acetyl, hydroxymethyl, carboxylate, and methyl side chains and two packing parameters (μ, w) for positioning each double helix in the unit cell. Conformation angles (ϕ, ψ) around the glycosidic bonds of the polyanion were elastically tethered to appropriate standard values, which were chosen from the corresponding hard sphere map of each disaccharide unit. The cations and periodic water molecules were located by examining difference Fourier maps computed using $(2F_o - F_c)$ as coefficients in which the F_c and its phase were derived for the current model corresponding to normal atomic scattering factors[20]. Three parameters defining the position of each Ca^{2+} ion and water molecule were additional variables in the crystal-structure refinement. These refinements and the reported R-values are based on water-smeared scattering factors[21].

DEVELOPMENT OF THE CRYSTAL STRUCTURE

According to the measured fiber density of 1.49 g/mL, the unit cell of welan could accommodate three double helices. In addition, there could be up to one Ca^{2+} ion on average to neutralize the charge on a pair of carboxylate groups and about ten water molecules associated with each pentasaccharide repeating-unit. One would therefore expect that the resulting packing arrangement would be

significantly different from that of two double helices in the unit cell of the K^+ gellan crystal structure[15].

If two welan double helices, I and II, are positioned such that their (u, v) values are (2/3, 1/3) and (1/3, 2/3), respectively, as in the K^+ gellan crystal structure, there is substantial space for a third double helix III at (0, 0) of the unit cell. Also a two-dimensional electron density map computed using the F_o's of $hk0$ reflections and phases derived from I and II alone showed a strong peak around (0, 0) that could represent the third double helix. Whether the polarity of a helix is "up" or "down" has to be determined at each site. Many of the $2^3 = 8$ possible combinations, however, are not independent. For example, all "up" is the same as all "down", and likewise, two "up" and one "down" is the same as one "up" and two "down". Taking into account these redundancies, the number of cases to be investigated reduces to two. The first is the all "up" and the second, two "up" and one "down". These are henceforth denoted as the "parallel" (model P) and "antiparallel" (model A) packing arrangements, respectively. In the second case, II was chosen as the "down" double helix for easy comparison with the K^+ gellan structure. Both cases correspond to the space group $P3_1$ and the five packing parameters described below have to be determined in each case.

By treating the double helix as a rigid body, the probable values of the packing parameters were determined for each model by conducting surveys of the nonbonded contacts among double helices I, II, and III in the five-dimensional (μ, w) space (i.e., μ_1 for I, μ_2 and w_2 for II, and μ_3 and w_3 for III), where the variables μ and ω were scanned at intervals of 20° and 0.05, respectively. The surveys provided only the probable ranges of the packing parameters and it was difficult to fix unambiguously the orientations of the three helices. However, for some reasonable values within these ranges, $(2F_o - F_c)$ maps were computed for both models. The R-value at this stage was ~ 0.46 for model A. Both maps clearly showed two strong peaks in the vicinity of carboxylate groups, one located between I and III and the other between II and III. Assuming that these peaks were possible sites for Ca^{2+} ions, the packing parameters were adjusted manually so that there could be $COO^- \cdots Ca^{2+} \cdots COO^-$ interactions between I and III and between II and III. For example, in the case of model A, μ_1 and μ_2 were changed by 15° and −58° and w_2 by −0.40 from the corresponding gellan values[15]. The packing parameters and scale factor for each model containing only the three welan double helices were then refined against the X-ray data and intermolecular steric repulsion. This gave R-values of 0.37 for model A and 0.39 for model P for a total of 91 reflections. This small difference was not helpful to discriminate one over the other. Therefore, both models were further examined for the purpose of locating cations and water molecules.

Choosing the correct packing model.—The second $(2F_o - F_c)$ map for model A indicated that the adjustment of packing parameters was compatible with the right molecular orientations, and the side chain and the acetyl group were in the correct orientations. The map also confirmed the two strong peaks previously seen in the

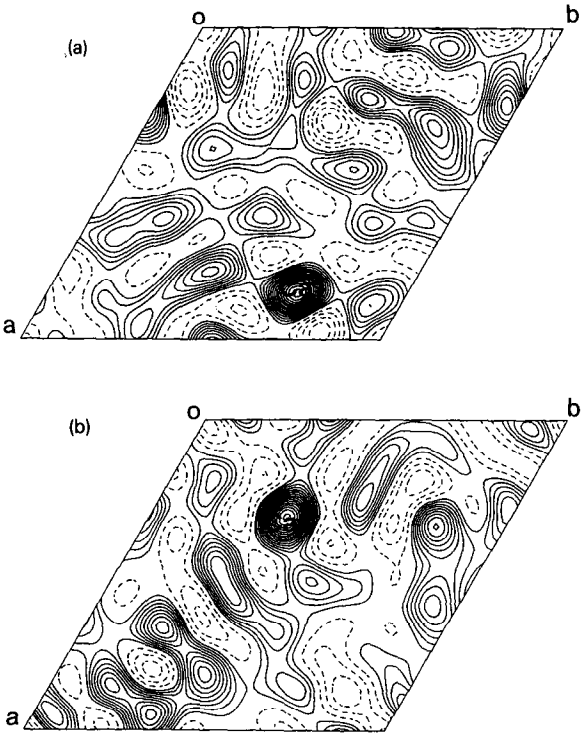

Fig. 2. Three-dimensional $(2F_o - F_c)$ map for sections (a) $14c/31$ and (b) $-2c/31$. The strongest peaks, marked Ca1 and Ca2, correspond to the two calcium ions in the crystallographic asymmetric unit.

first map, one located between the carboxylate groups of I and III (Fig. 2a), the other between the carboxylate groups of II and III (Fig. 2b). Calcium ions Ca-1 and Ca-2 were placed at these two positions. Seven more peaks surrounding the polyanions were selected as oxygen atoms representing water molecules. Their positions, as well as the packing parameters of the polyanions, and the X-ray scale factor were simultaneously refined and this gave an R-value of 0.27. Further refinement of the augmented crystal structure, followed by three subsequent difference Fourier maps, led to a total of 25 water molecules located in a third of

TABLE I

Statistics for the antiparallel (model A) and parallel (model P) packing arrangements of welan based on X-ray data and non-bonded contacts [a]

Model	N_X	X	N_C	C	Ω	$(\Omega/\Omega_A)^{1/2}$	R
A	103	36	216	16	52	1.000	0.225
P	101	45	211	22	67	1.135	0.259

[a] The function minimized in the least-squares procedure[19] is given by $\Omega = X + C$ where $X = \Sigma w_m ({}_oF_m - F_m)^2$ and $C = \Sigma k_j ({}_od_j - d_j)^2$ are respectively the X-ray and steric repulsion terms; N_X and N_C are the corresponding number of observations. R is the crystallographic reliability index.

TABLE II

Cartesian and cylindrical polar atomic coordinates for an asymmetric unit of calcium welan consisting of a pentasaccharide[a] in one chain, the associated cations, and water molecules

Group	Atom	x(Å)	y(Å)	z(Å)	r(Å)	ϕ(°)
Residue A	C-1	−1.0853	−2.6319	15.3916	2.8469	−112.41
	C-2	−0.7168	−2.3143	16.8348	2.4228	−107.21
	C-3	−1.7505	−2.8937	17.7884	3.3820	−121.17
	C-4	−3.1426	−2.4127	17.4007	3.9619	−142.49
	C-5	−3.4054	−2.7025	15.9267	4.3474	−141.56
	C-6	−4.7279	−2.1423	15.4479	5.1906	−155.62
	C-7	1.1465	−2.5276	18.2717	2.7755	−65.60
	C-8	2.2173	−3.5330	18.6263	4.1712	−57.89
	O-2	0.5776	−2.8348	17.1151	2.8930	−78.48
	O-3	−1.4426	−2.4988	19.1267	2.8853	−120.00
	O-4	−4.1336	−3.0788	18.1800	5.1542	−143.32
	O-5	−2.3851	−2.1099	15.1082	3.1844	−138.50
	O-6	−5.8354	−2.8534	15.9993	6.4957	−153.94
	O-7	0.8246	−1.5560	18.9355	1.7610	−62.08
	H-1	−1.0878	−3.7221	15.2448	3.8778	−106.29
	H-2	−0.6639	−1.2237	16.9684	1.3922	−118.48
	H-3	−1.7134	−3.9904	17.7118	4.3427	−113.24
	H-4	−3.2206	−1.3306	17.5826	3.4847	−157.55
	H-5	−3.4176	−3.7902	15.7633	5.1035	−132.04
	H-61	−4.7987	−1.0804	15.7260	4.9188	−167.31
	H-62	−4.7708	−2.1907	14.3499	5.2497	−155.34
	H-81	3.0564	−3.4394	17.9212	4.6012	−48.37
	H-82	2.5750	−3.3427	19.6490	4.2195	−52.39
	H-83	1.8004	−4.5493	18.5670	4.8926	−68.41
Residue B	C-1	0.6737	−2.2172	10.4993	2.3173	−73.10
	C-2	−0.6899	−2.7452	10.9249	2.8306	−104.11
	C-3	−1.0434	−2.2043	12.3018	2.4388	−115.33
	C-4	0.0555	−2.5812	13.2866	2.5818	−88.77
	C-5	1.4083	−2.1069	12.7663	2.5342	−56.24
	C-6	2.5613	−2.5624	13.6360	3.6230	−15.01
	O-2	−1.6660	−2.3538	9.9663	2.8837	−125.29
	O-3	−2.2588	−2.8038	12.7549	3.6005	−128.86
	O-4	−0.1872	−1.9798	14.5565	1.9886	−95.40
	O-5	1.6593	−2.6245	11.4506	3.1050	−57.70
	O-61	2.4734	−3.7011	14.1441	4.4515	−56.25
	O-62	3.5132	−1.7651	13.7796	3.9317	−26.68
	H-1	0.6426	−1.1187	10.4508	1.2901	−60.13
	H-2	−0.6663	−3.8447	10.9491	3.9020	−99.83
	H-3	−1.1450	−1.1101	12.2511	1.5948	−135.89
	H-4	0.0707	−3.6757	13.3959	3.6764	−88.90
	H-5	1.4227	−1.0075	12.7309	1.7433	−35.31
Residue C	C-1	1.4988	−1.4889	5.4230	2.1126	−44.81
	C-2	1.5328	−0.3846	6.4713	1.5803	−14.08
	C-3	1.7751	−1.0168	7.8333	2.0457	−29.80
	C-4	0.6925	−2.0515	8.1106	2.1652	−71.35
	C-5	0.5809	−3.0417	6.9562	3.0967	−79.19
	C-6	−0.5934	−3.9853	7.1073	4.0292	−98.47
	O-2	2.5498	0.5522	6.1349	2.6089	12.22

TABLE II (continued)

Group	Atom	x(Å)	y(Å)	z(Å)	r(Å)	φ(°)
Residue C	O-3	1.7585	−0.0044	8.8416	1.7585	−0.14
	O-4	1.0081	−2.7991	9.2832	2.9751	−70.19
	O-5	0.3949	−2.3489	5.7122	2.3819	−80.46
	O-6	−1.8010	−3.4127	6.6070	3.8588	−117.82
	H-1	2.4335	−2.0680	5.4558	3.1935	−40.36
	H-2	0.5761	0.1583	6.4634	0.5975	15.37
	H-3	2.7649	−1.4968	7.8441	3.1440	−28.43
	H-4	−0.2651	−1.5298	8.2548	1.5526	−99.83
	H-5	1.4983	−3.6464	6.9016	3.9422	−67.66
	H-61	−0.3822	−4.9225	6.5715	4.9373	−94.44
	H-62	−0.7221	−4.2437	8.1687	4.3047	−99.66
Residue D	C-1	3.8234	0.1411	1.0349	3.8260	2.11
	C-2	3.3521	1.2340	1.9859	3.5720	20.21
	C-3	2.0826	0.7806	2.6923	2.2241	20.55
	C-4	2.4172	−0.4893	3.4617	2.4662	−11.44
	C-5	2.8878	−1.5570	2.4634	3.2808	−28.33
	C-6	3.3255	−2.8496	3.1264	4.3794	−40.59
	O-2	4.4029	1.4822	2.9109	4.6457	18.61
	O-3	1.6577	1.8519	3.5124	2.4855	48.17
	O-4	1.2635	−0.9190	4.1783	1.5624	−36.03
	O-5	4.0296	−1.0775	1.7323	4.1712	−14.97
	H-1	4.7585	0.4441	0.5413	4.7792	5.33
	H-2	3.1572	2.1556	1.4179	3.8229	34.32
	H-3	1.3008	0.5759	1.9462	1.4226	23.88
	H-4	3.2299	−0.2728	4.1707	3.2414	−4.83
	H-5	2.0763	−1.7799	1.7550	2.7348	−40.60
	H-61	2.4460	−3.4846	3.3085	4.2574	−54.93
	H-62	4.0299	−3.3792	2.4682	5.2592	−39.98
	H-63	3.8180	−2.6225	4.0834	4.6319	−34.48
Residue E	C-1	2.8549	0.8722	8.8685	2.9852	16.99
	C-2	2.9646	1.4888	10.2579	3.3174	26.67
	C-3	3.3215	0.4057	11.2658	3.3462	6.96
	C-4	4.6570	−0.1880	10.8408	4.6608	−2.31
	C-5	4.5012	−0.7916	9.4370	4.5703	−9.97
	C-6	5.7961	−1.3449	8.8728	5.9501	−13.06
	O-2	3.9628	2.5000	10.2025	4.6855	32.25
	O-3	3.3453	1.0160	12.5411	3.4962	16.89
	O-4	5.0284	−1.2095	11.7615	5.1718	−13.53
	O-5	4.0636	0.2194	8.5127	4.0695	3.09
	O-6	5.5595	−2.2738	7.8157	6.0065	−22.24
	H-1	2.6260	1.6505	8.1257	3.1016	32.15
	H-2	2.0056	1.9545	10.5292	2.8005	44.26
	H-3	2.5709	−0.3973	11.2224	2.6014	−8.78
	H-4	5.4097	0.6135	10.8096	5.4444	6.47
	H-5	3.7543	−1.5986	9.4655	4.0805	23.06
	H-61	6.3820	−0.5266	8.4287	6.4037	−1.72
	H-62	6.3643	−1.8387	9.6748	6.6246	−16.11
	H-63	5.5700	2.0545	8.0632	5.9368	−20.25
Calcium	Ca-1	14.8132	5.7249	11.9002	15.8810	21.13
	Ca-2	5.1798	3.9317	−2.0908	6.5030	37.20

TABLE II (continued)

Group	Atom	x(Å)	y(Å)	z(Å)	r(Å)	φ(°)
Water	W1	5.7010	−1.7332	−4.5034	5.9586	−16.91
	W2	2.9911	−5.2845	−0.3567	6.0723	−60.49
	W3	4.9621	3.4372	6.9926	6.0363	−34.71
	W4	5.3044	1.4342	−0.2313	5.4949	15.13
	W5	6.2925	4.2380	0.6800	7.5866	33.96
	W6	2.5727	5.5960	−2.5570	6.1590	65.31
	W7	6.7019	4.6875	−4.6010	8.1785	34.97
	W8	8.9551	14.8275	−0.5489	17.3219	58.87
	W9	3.2370	15.2813	−2.67161	5.6204	78.04
	W10	5.2535	−4.8123	−4.4408	7.1244	−42.49
	W11	0.5737	−9.2729	−3.7123	9.2906	−86.46
	W12	17.0138	−4.0721	−4.6400	17.4943	−13.46
	W13	8.0834	−5.2294	−3.8258	9.6274	−32.90
	W14	0.6369	14.3565	−3.0339	14.3706	87.46
	W15	6.0154	1.0488	2.9852	6.1061	9.89
	W16	4.9314	2.3385	0.9625	5.4578	25.37
	W17	6.0441	1.4969	−1.4244	6.2267	13.91
	W18	6.5880	4.0339	−6.7604	7.7249	31.48
	W19	5.2111	2.0453	−8.5742	5.5981	21.43
	W20	5.6048	2.0002	−5.7823	5.9510	19.64
	W21	0.2529	−8.8336	−4.5266	8.8372	−88.36
	W22	12.7843	14.6034	1.7540	19.4087	48.80
	W23	12.6229	11.7217	−0.8144	17.2260	42.88
	W24	11.2832	14.7258	6.5697	18.5515	52.54
	W25	6.0336	−2.8431	−1.1962	6.6699	−25.23

[a] The next two pentasaccharides in the chain are generated as $(r, \phi - 120°, z + 2c/3)$, and $(r, \phi + 120°, z + 4c/3)$. The second chain in the double helix is generated from the first by adding c to the corresponding z coordinates. For a down-pointing double helix, the atomic coordinates are $(r, -\phi, -z)$. The following packing parameters are to be applied to these coordinates to generate the crystal structure whose space group symmetry is $P3_1$.

Molecule	Sense	μ	u	v	w
I	up	107.9°	2/3	1/3	0.0
II	down	−125.0°	1/3	2/3	0.4083
III	up	45.6°	0	0	0.4328
Ca and water		0.0°	0	0	0.0

the unit cell. This volume constitutes the crystallographic asymmetric unit and contains three pentasaccharide units, one from each double helix.

Similar steps were followed to locate Ca^{2+} ions and water molecules in model P. Two Ca^{2+} ions located between the double helices and 25 water molecules, all having atomic coordinates similar to those in model A, except for two, could be located in a series of $(2F_o - F_c)$ maps.

Subsequently, the positions of cations and water molecules were refined for each model along with the packing parameters of the double helices. At the end of the refinement, the R-values reached 0.225 for model A and 0.259 for model P and their statistics are compared in Table I. Application of Hamilton's significance

test[22], based on the overall term Ω suggests that model A is indeed superior to model P at 99.5% confidence level. Similarly, the X-ray term X or R-value is sufficient to establish significant superiority of model A over model P. Therefore, model A was chosen as the best representation of the crystal structure of Ca^{2+} welan.

TABLE III

(A) Scaled observed and (B) calculated structure amplitudes for calcium welan [a]

A

h	k	l=0	1	2	3	4	5	6	7	8	9	10	11
0	0	M	N	N	M	N	N	M	N	N	M	N	N
1	0	253	169	(56)	(59)	68	288	278	218	N	N	N	N
1	1	401	(79)	252	160	100	[91]	(99)	229				
2	0	237	289	(85)	104	115	(102)	(106)	(116)	501	346	332	N
2	1	(100)	292	279	126	245	173	249	367	284	320	303	297
3	0	229	337	316	(121)	272	194	247	(152)	[163]	(179)	(194)	343
2	2	454	461	(134)	[136]	310							
3	1	566	509	419	412	307	422	446	425	452	346	325	294
4	0	754	358	(154)	(153)	231	306	(183)	(195)	[206]	(224)	[245]	[269]
3	2	668	332	613	(172)	(178)	(185)						
4	1	888	464	538	280	234		351	400	381	413		
5	0	491	515	363	(201)	(209)		[227]	[240]	[259]	[278]		
3	3												
4	2	431	508	349									
5	1	218	(222)	(222)									
4	3	393											
5	2	416											
6	1	(282)											

B

h	k	l=0	1	2	3	4	5	6	7	8	9	10	11
0	0	[1857]	[0]	[0]	[38]	[0]	[0]	[98]	[0]	[0]	[319]	[0]	[0]
1	0	92	203	(195)	(93)	95	124	145	175	[0]	[0]	[0]	[0]
1	1	345	(146)	241	161	164	[64]	(70)	180				
2	0	240	147	(180)	103	121	(168)	(206)	(132)	406	281	376	[0]
2	1	(308)	183	263	236	227	297	210	305	251	275	333	274
3	0	381	272	161	(223)	238	141	275	(159)	[145]	(208)	(250)	330
2	2	699	431	(192)	[95]	187							
3	1	507	405	405	373	282	428	419	314	400	401	337	362
4	0	444	465	(240)	(173)	292	288	(183)	(209)	[160]	(255)	[193]	(181)
3	2	528	386	534	(193)	[181]	(246)						
4	1	907	537	349	325	220		395	374	393	419		
5	0	354	342	222	(241)	(216)		[197]	[133]	[89]	[159]		
3	3												
4	2	481	592	465									
5	1	152	(228)	(308)									
4	3	378											
5	2	389											
6	1	(288)											

[a] Amplitudes in parentheses indicate reflections below the threshold of observation, and their estimated threshold values are given in A. The curved and rectangular brackets refer, respectively, to reflections included in, and rejected from, the least-squares refinement. M denotes meridional reflection, N systematically absent or unobserved reflection, respectively. The final value of the attenuation factor is 4.7 Å^2.

Final refinement was conducted for this model such that the attenuation factor B, previously held at 6 Å^2, was also allowed to vary along with the molecular parameters. This produced marginal shifts in the conformational and packing parameters and a slight drop in R-value to 0.215 for a total of 102 reflections. The atomic coordinates of this model are given in Table II. The observed and calculated structure amplitudes are listed in Table III.

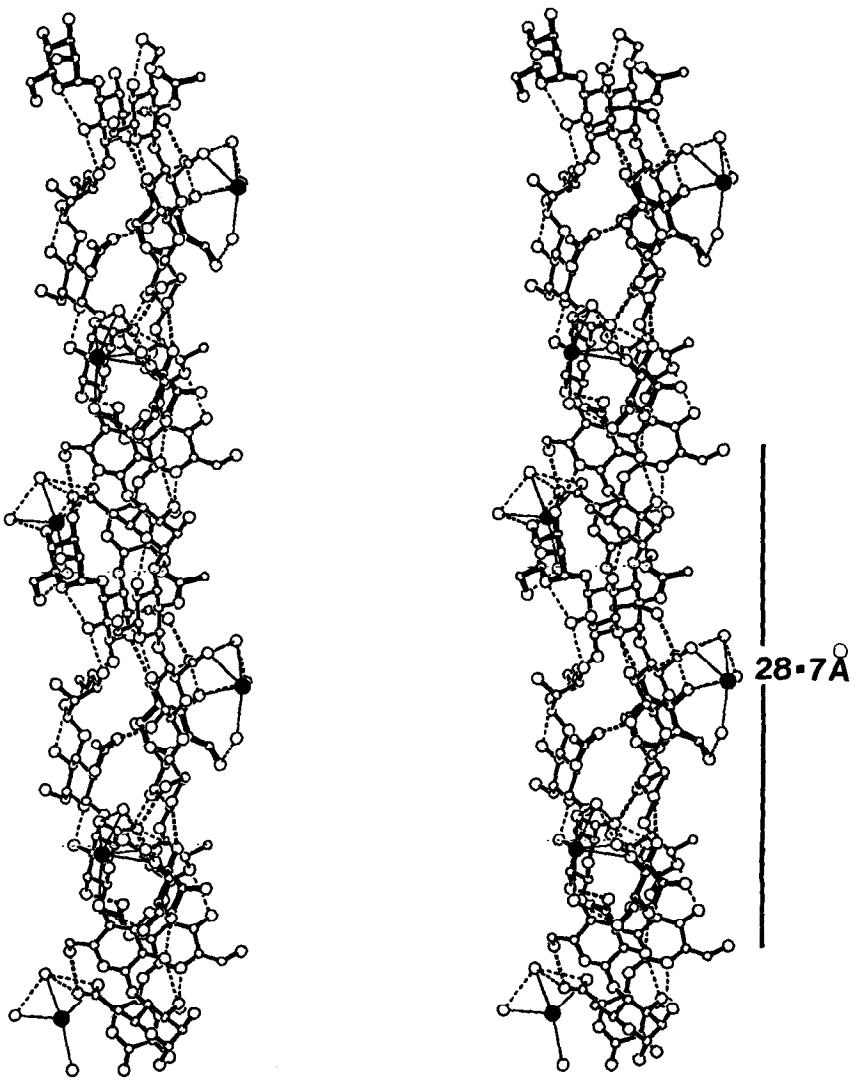

Fig. 3. A stereo view of the welan double helix. Side chains and acetyl groups are accentuated by thick bonds. Hydrogen bonds within a chain (thin dashed lines) and between the chains (thick dashed lines), and contacts marked by thin lines between calcium ions (filled circles), water molecules (unfilled circles) and the helix are responsible for the stability of the welan molecule.

STRUCTURAL FEATURES

Polyanion conformation.—The main chain of welan has three-fold helix symmetry with a left-handed twist. A side view of the double helix (Fig. 3) shows that the molecule is fairly extended. The peripheral side chains fold back on the main chain toward the reducing end, exactly as predicted earlier[14]. Both intra- and inter-chain hydrogen bonds involving functional groups in the main and side chains provide stiffness and stability to the welan double helix whose conformation angles are listed in Table IV. While the structural features of welan are presented in this section, their comparison with gellan and native gellan, and implications to functional properties will be described in a later section. Along the main chain of welan, (ϕ_2, ψ_2) and (ϕ_3, ψ_3) have some resemblance to those (−98°, −142°) of cellulose, except for a large difference of about −49° for ϕ_3.

The oxygen atoms of hydroxymethyl groups in the glucosyl units take up *gauche* positions such that χ_1 is −70° in residue A and χ_3 is 85° in residue C. On the other hand, atom O-6 of residue E has *trans* orientation and χ_5 is 161°. The carboxylate group in the glucuronate residue has $\chi_2 = 37°$ and corresponds to a *cis* conformation.

Inspection of the radial atomic coordinates in Table II indicates that atoms belonging to residues A, D, and E at $r = 6.5$, 5.2, and 6.6 Å, respectively, describe the periphery of the molecule, the terminal hydrogen atom H-62E being farthest from the helix axis; in contrast, atoms of B and C at $r = 4.3$ and 4.9 Å, respectively, are closer to the helix axis and define the inner core. The acetyl moiety, located in

TABLE IV

Comparison of conformation angles in (*a*) calcium welan (esd) with (*b*) computer generated model of K^+ welan [a], and (*c*) potassium native gellan[24]

Conformation angle (°)	*a*	*b*	*c*	Remarks
ϕ_1(O-5D–C-1D–O-3A–C-3A)	−104(1)	−124	−119	α-(1 → 3)
ψ_1(C-1D–O-3A–C-3A–C-4A)	90(1)	88	64	α-(1 → 3)
χ_1(C-4A–C-5A–C-6A–O-6A)	−70(3)	−79	−82	hydroxymethyl
θ_1(C-1A–C-2A–O-2A–C-7A)	171(2)			acetyl
θ_2(C-2A–O-2A–C-7A–O-7A)	−23(2)			acetyl
θ_3(O-2A–C-7A–C-8A–H-81A)	−172(2)			acetyl
ϕ_2(O-5A–C-1A–O-4B–C-4B)	−90(1)	−101	−99	β-(1 → 4)
ψ_2(C-1A–O-4B–C-4B–C-5B)	−157(1)	−136	−150	β-(1 → 4)
χ_2(C-4B–C-5B–C-6B–O-61B)	37(3)	10	24	carboxylate
ϕ_3(O-5B–C-1B–O-4C–C-4C)	−147(1)	−154	−134	β-(1 → 4)
ψ_3(C-1B–O-4C–C-4C–C-5C)	−157(1)	−144	−148	β-(1 → 4)
χ_3(C-4C–C-5C–C-6C–O-6C)	85(3)	58	62	hydroxymethyl
ϕ_4(O-5C–C-1C–O-4D–C-4D)	−155(1)	−150	−141	β-(1 → 4)
ψ_4(C-1C–O-4D–C-4D–C-5D)	96(1)	86	98	β-(1 → 4)
χ_4(C-4D–C-5D–C-6D–H-61D)	84(3)	77	91	methyl
ϕ_5(O-5E–C-1E–O-3C–C-3C)	−35(2)	−37		side chain
ψ_5(C-1E–O-3C–C-3C–C-2C)	−71(1)	−74		side chain
χ_5(C-4E–C-5E–C-6E–O-6E)	161(3)			side chain

[a] K^+ welan model[14] incorporates the same conformation angles as in K^+ gellan fibers[15].

the interior of the helix, exhibits no bad contacts within or between the polymer chains and does not appear to have any destabilizing effect on the double helix.

Among the four local turn angles of the helix (Table V), calculated as the differences in the cylindrical polar angles ϕ of adjacent bridge oxygen atoms, those of residues A (−24.5°) and B (−25.3°) are less, but C (−34.2°) and D (−36.0°) are more than the average value of −30° per residue. The projected lengths of adjacent bridge oxygen atoms along the helix axis show different trends; the values for B (5.3 Å) and C (5.1 Å) are larger than for D (4.2 Å) and A (4.6 Å). In cellulose[23], which has an extended chain conformation, the axial rise is 5.2 Å.

Intrachain hydrogen bonds.—The welan chain derives stability through six intrachain hydrogen bonds (Table VI) per pentasaccharide repeating unit. There is at least one hydrogen bond across every bridge oxygen atom except for O-4C. Notable is the cellulosic hydrogen bond O-3B · · · O-5A. Although there is no link between residues B and C, such as O-2B · · · O-6C in gellan, side chain E generates three hydrogen bonds O-3E · · · O-62B, O-4E · · · O-62B, and O-2C · · · O-5E and thus lends additional molecular stability. The first two hydrogen bonds are consistent with predictions from the computer modeling study[14].

Interchain hydrogen bonds.—The juxtaposition of the interstrand pairs A and C, B and D, and E and C (Fig. 3) facilitates the formation of not only the gellan-like O-6C · · · O-62B interchain hydrogen bond, but also O-3E · · · O-5C and O-2B · · · O-7A interchain hydrogen bonds involving the side chain and acetyl group, respectively, and are listed in Table VI. Thus the welan double helix is stabilized by three interchain hydrogen bonds instead of only one in the case of gellan. The hydroxyl groups of the rhamnosyl unit (D) do not contribute to the interchain hydrogen-bonding scheme. All the hydrogen bonds within a double helix are schematically represented in Fig. 4.

Calcium ions and water molecules.—Two carboxylate groups from adjoining double helices are utilized in counter-balancing the charge on the Ca^{2+} ions. However, the two ions, Ca-1 and Ca-2, have quite different surroundings. Ca-1 is surrounded by a total of seven neighbors (Table VI) which include atoms O-61B, O-62B, and O-4E in one chain of double helix I, O-6E in one chain of III, and three water molecules W1, W2, and W3. Among them, W1 is hydrogen bonded to O-61B of III and leads to a series of $COO^- \cdots Ca^{2+} \cdots W \cdots COO^-$ interac-

TABLE V

Local turn angles and axial rises in (*a*) welan compared with those of (*b*) K^+ gellan, and (*c*) K^+ native gellan

Residue	Turn angle (°)			Axial rise (Å)		
	a	*b*	*c*	*a*	*b*	*c*
Glucose (A)	−24.5	−0.6	−3.8	4.6	4.6	4.7
Glucuronate (B)	−25.3	−64.6	−49.8	5.3	4.8	5.0
Glucose (C)	−34.2	−39.8	−43.1	5.1	5.2	5.1
Rhamnose (D)	−36.0	−15.1	−23.3	4.2	4.1	4.2

TABLE VI

Attractive interactions in the crystal structure of calcium welan including calcium ions and water molecules [a]

Type	Atom X	Atom Y	X ··· Y (Å)	Precursor P	P–X ··· Y (°)
Intrachain	O-3B	O-5A	2.46	C-3B	103
	O-4A	O-5D	2.93	C-4A	101
	O-3D	O-2C	3.06	C-3D	95
	O-3E	O-62B	3.04	C-3E	89
	O-4E	O-62B	2.58	C-4E	120
	O-2C	O-5E	2.84	C-2C	96
Interchain	O-6C	O-62B	3.08	C-6C	147
	O-3E	O-5C	3.16	C-3E	147
	O-2B	O-7A	2.49	C-2A	117
Inter double helix	O-2E(I,1)	O-6A(III,1)	2.82	C-2E	113
	O-4E(I,1)	O-2E(II,2)	3.15	C-4E	82
	O-4E(II,1)	O-6C(III,1)	3.14	C-4E	110
Calcium environment	O-61B(I,1)	Ca-1	3.17	C-6B	83
	O-62B(I,1)	Ca-1	3.42	C-6B	72
	O-4E(I,1)	Ca-1	3.24	C-4E	135
	O-6E(III,2)	Ca-1	3.09	C-6E	104
	W1	Ca-1	3.01		
	W2	Ca-1	2.76		
	W3	Ca-1	3.08		
	O-61B(II,1)	Ca-2	3.40	C-6B	73
	O-62B(II,1)	Ca-2	2.61	C-6B	111
	O-4E(II,1)	Ca-2	2.85	C-4E	174
	O-62B(III,2)	Ca-2	3.06	C-6B	156
	O-4E(III,2)	Ca-2	2.82	C-4E	128
	W4	Ca-2	3.11		
	W5	Ca-2	3.00		
	W6	Ca-2	3.13		
	W7	Ca-2	3.03		
Water bridges					
Intrachain	O-3D(II,1)	W8	3.01	C-3D	114
	O-2D(II,1)	W8	3.43	C-2D	77
	O-5D(II,1)	W9	3.14	C-5D	93
	O-2D(II,1)	W9	2.96	C-2D	127
	O-5E(II,1)	W10	2.76	C-1E	110
	O-2C(II,1)	W10	3.10	C-2C	149
	W1	W10	3.11		
	W9	W10	2.79		
	O-2C(I,1)	W11	3.07	C-2C	128
	O-6E(I,1)	W11	3.03	C-6E	89
	O-5E(I,1)	W11	3.07	C-1E	132
Interchain	O-6C(III,1)	W4	3.06	C-6C	158
	O-61B(III,2)	W4	3.09	C-6B	86
	O-62B(III,2)	W4	2.77	C-6B	101
Inter double helix	O-61B(III,1)	W1	2.87	C-6B	99
	O-5B(III,1)	W1	2.90	C-5B	107
	O-61B(I,2)	W1	3.09	C-6B	87
	O-62B(I,2)	W1	2.82	C-6B	100
	O-6E(III,1)	W2	2.89	C-6E	158
	O-6E(I,2)	W2	2.95	C-6E	102
	W22	W2	2.88		
	W10	W3	2.91		

TABLE VI (continued)

Type	Atom X	Atom Y	X ··· Y (Å)	Precursor P	P–X ··· Y (°)
Inter double helix	W1	W3	3.11		
	O-4E(I,2)	W3	2.87	C-4E	136
	O-2E(II,1)	W3	3.05	C-2E	123
	W4	W5	3.11		
	O-4E(II,1)	W5	2.67	C-4E	120
	O-62B(II,1)	W6	3.05	C-6B	176
	O-6C(II,1)	W6	2.81	C-6C	109
	O-3E(II,1)	W6	3.19	C-3E	112
	O-4E(II,1)	W6	2.94	C-4E	109
	O-3E(III,2)	W6	2.92	C-3E	122
	O-4E(III,2)	W7	3.03	C-4E	108
	O-61B(II,1)	W7	2.83	C-6B	108
	W14	W9	2.78		
	O-6E(I,1)	W12	2.97	C-6E	149
	O-2E(III,2)	W12	3.04	C-2E	125
	W11	W12	3.10		
	O-6C(I,1)	W13	2.84	C-6C	92
	W10	W13	2.92		
	O-6E(II,1)	W14	2.81	C-6E	153
	O-3B(III,1)	W14	2.95	C-3B	156
	W21	W14	2.82		
	W4	W15	3.32		
	O-2E(III,1)	W16	2.73	C-2E	111
	W17	W16	2.77		
	O-2D(III,1)	W17	2.99	C-2D	152
	O-3B(II,2)	W17	2.98	C-3B	116
	W23	W17	2.94		
	W19	W18	3.03		
	W20	W18	2.46		
	O-3B(I,1)	W18	2.85	C-3B	149
	O-2A(III,1)	W19	2.74	C-2A	112
	W25	W19	2.81		
	O-2D(II,1)	W19	3.10	C-2D	104
	O-2D(III,1)	W20	2.76	C-2D	78
	W19	W20	2.83		
	O-2D(I,1)	W21	2.89	C-2D	157
	O-6E(II,1)	W21	3.06	C-6E	148
	W11	W21	2.96		
	O-6A(II,1)	W22	2.95	C-6A	96
	O-6E(III,1)	W22	2.96	C-6E	142
	W23	W22	3.04		
	O-2C(III,1)	W23	3.07	C-2C	128
	O-5E(III,1)	W23	3.02	C-1E	132
	O-6E(III,1)	W23	3.04	C-6E	88
	O-3B(II,1)	W23	3.21	C-3B	156
	O-4A(II,1)	W24	2.72	C-4A	115
	O-6A(II,1)	W24	2.60	C-6A	111
	O-3E(I,1)	W24	3.04	C-3E	112
	O-2E(I,1)	W24	2.79	C-2E	120
	O-4A(III,1)	W24	3.11	C-4A	160
	O-61B(III,1)	W25	2.78	C-6B	175
	O-2D(II,1)	W25	3.03	C-2D	142

[a] I, II, and III, or 1 and 2, in parentheses after the atom name refer to the three double helices in the unit cell, or the two chains in a double helix.

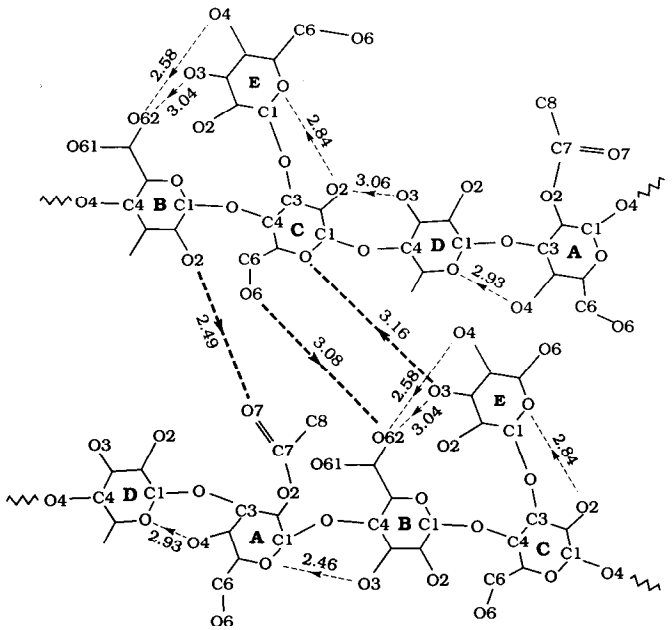

Fig. 4. A schematic illustration of the six intra- (thin dashed lines) and three inter-chain (thick dashed lines) hydrogen bonds in a repeating unit of the welan double helix. Distances are given in Å.

tions. In contrast, Ca-2 has nine neighbors. They are atoms O-61B, O-62B and O-4E in one chain of II, O-62B and O-4E in one strand of III, and four water molecules W4, W5, W6, and W7. This set up establishes direct $COO^- \cdots Ca^{2+} \cdots COO^-$ interactions.

Molecular packing.—Welan molecules are connected by either side chain–main chain or side chain–side chain hydrogen-bonds and there is one occurring in every repeating unit. Of the three hydrogen bonds possible (Table VI), atoms O-2E and O-4E are donors and O-6A and O-6C are the corresponding acceptors in two cases and the third hydrogen bond O-4E $\cdots$ O-2E involves exclusively side chain atoms. These observations suggest that side chains are extremely important for the lateral organization and stability of welan double helices.

The packing arrangement of the three double helices in the unit cell, as viewed along the *c*-axis, is shown in Fig. 5. Each helix is surrounded by six similar neighbors, at the corners of a hexagon of side 12.0 Å. The six calcium ions in the unit cell are located in the gaps between the helices in the vicinity of the carboxylate groups. There are three distinct types of intermolecular interactions which are brought out by the guest molecules. For example, double helices I and II, arranged antiparallel as in gellan, are not connected by calcium ions, but are linked only by side chain–side chain hydrogen bonds (Fig. 6a). Double helices I and III, which are parallel, are connected by water-involving $COO^- \cdots Ca^{2+} \cdots W \cdots COO^-$ interactions besides inter double-helix hydrogen-bonds between

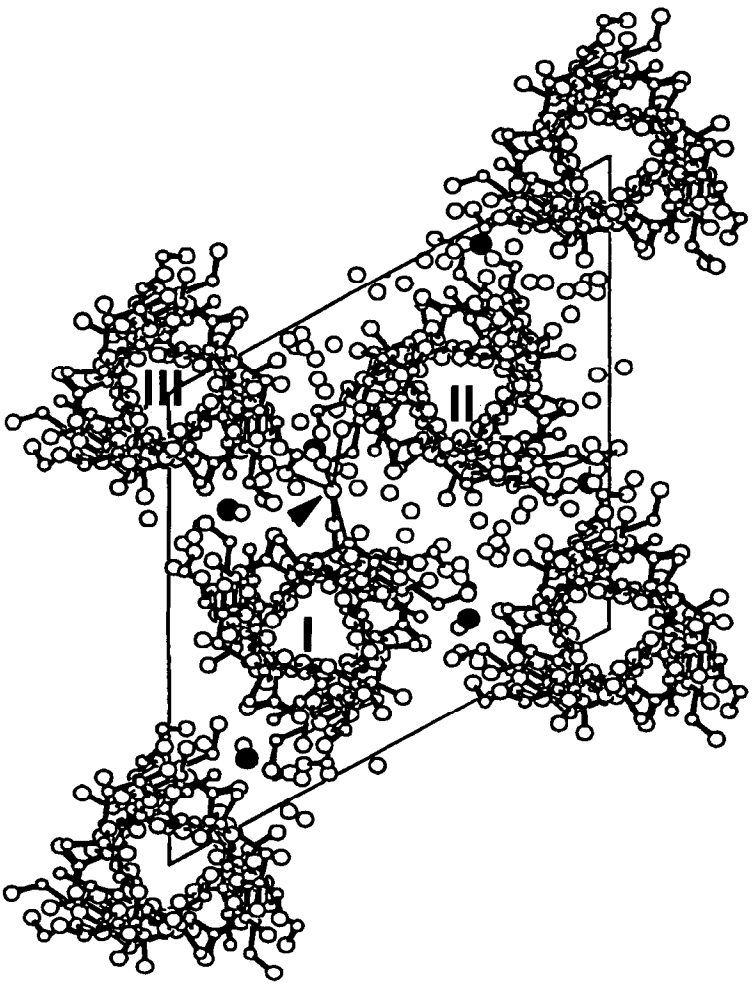

Fig. 5. A *c*-axis projection of the unit cell showing double helices I and III (both up) and II (down), calcium ions and water molecules. The carboxylate groups are highlighted by thick bonds to visualize their closeness to, and orientation towards the calcium ions. W24 (near the arrow) is linked to all three double helices.

residues A and E (Fig. 6b). The third pair of double helices II and III, which are antiparallel, are held together by direct $COO^- \cdots Ca^{2+} \cdots COO^-$ interactions in addition to the side chain–main chain hydrogen-bonds (Fig. 6c). Water molecules, about eight per pentasaccharide, are also extensively hydrogen bonded in the crystal structure. Every water molecule, except W15, is held in position by at least two hydrogen bonds with oxygen atoms in the polyanion and other water molecules; W15 is hydrogen bonded only to another water molecule, W4. On the basis of the observed hydrogen-bonding pattern (Table VI), these water molecules can be classified into three groups. In the first group are W8, W9, W10, and W11, which are involved only in intrachain water bridges within a polysaccharide chain. In the

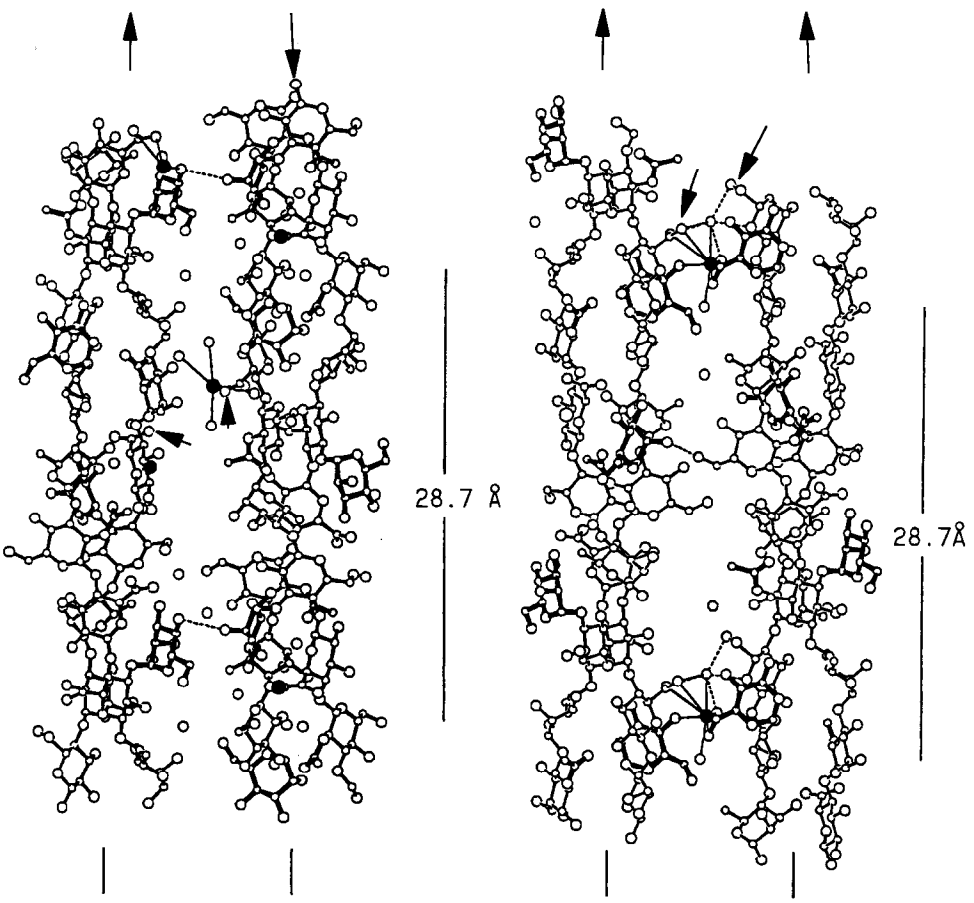

Fig. 6. Pairwise interactions between welan double helices in the unit cell, viewed perpendicular to intermolecular separation, involving calcium ions and water molecules: (a) I (up) and II (down), (b) I and III (both up), and (c) III (up) and II (down).

second group is W4, which is able to link both chains in III and acts as an interchain water bridge. The third group consists of the remaining water molecules, which take part in a series of double helix–water–double helix hydrogen bonds. Among them, W6 and W24 have as many as five hydrogen bonds. Further, W24 is unique in that it connects all three double helices directly as indicated in Fig. 5.

COMPARISON OF WELAN WITH GELLAN AND NATIVE GELLAN

Despite the acetyl groups and the side chains, welan retains the double helical structure (Fig. 3) that resembles the canonical gellan helix. However, the final conformation angles in welan (column 2 in Table IV) are not the same as the gellan values (listed in the next column) which were used to generate the molecu-

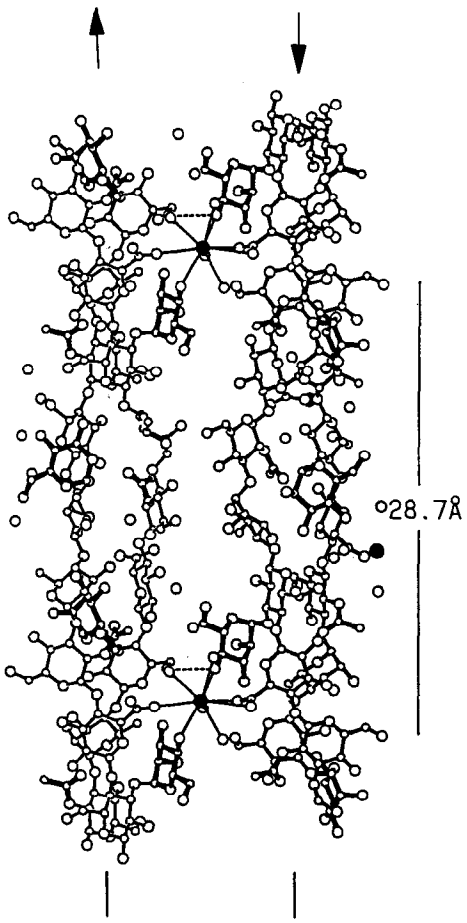

Fig. 6 (continued).

lar model[14] for K^+ welan. One of the reasons is the increase of pitch from 56.3 Å in K^+ gellan[15] to 57.4 Å in Ca^{2+} welan. The influence of substituents on morphology may be visualized by comparing the close-up views (Fig. 7) of one repeating unit in each strand and the associated cation in the three polymers including native gellan. Between the backbones of welan and gellan, conformation angles vary from 2° (for ψ_1) to 21° (for ψ_2). These changes might also be due to the cation positions not being the same in the two polymers. The value of $\phi_1 = -104°$ vs. $-124°$ in gellan is apparently due to the acetyl group on atom O-2A.

The differences between welan and gellan become more pronounced in the orientations of the hydroxymethyl and carboxylate groups. χ_2 in welan is 37°, 27° larger than in gellan. This additional rotation is needed for proper interaction of the carboxylate group with the divalent cation. Substantial movement of atom O-6C in welan ($\chi_3 = 85°$ vs. 58° in gellan) is equally necessary for preserving the interchain O-6C $\cdots$ O-62B hydrogen bond which stabilizes the double helix. A

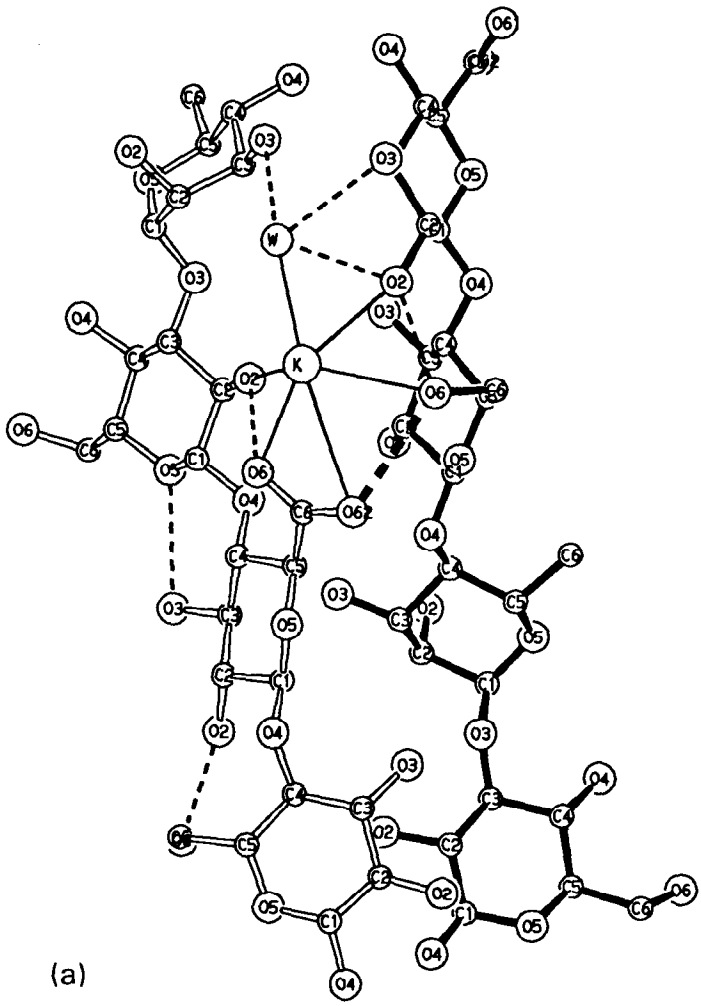

Fig. 7. A close-up, normal to the helix axis, of a repeating unit (all atoms labelled) per strand showing the influence of substitution and branching on the geometry of the double helix: (a) potassium gellan, (b) potassium native gellan, and (c) calcium welan.

majority of the conformation angles in native gellan[24] are intermediate to those of gellan and welan. A further reflection of the conformational differences is particularly seen in the local helical parameters (Table V). Residues A and D in welan turn around the helix axis much more, and residue B much less, than in gellan or native gellan and this leads to a more uniform distribution of turn angles for the four residues. It is interesting to note that the axial rise for residue A, and likewise for C or D, is virtually the same in the three polymers, but the rise for B increases progressively from gellan (4.8 Å) to native gellan (5.0 Å) and welan (5.3 Å) in the same way as the polysaccharide pitch increases from 56.3 to 56.8 and 57.4 Å. What appears to be a substitution effect on the main chain geometry can be understood

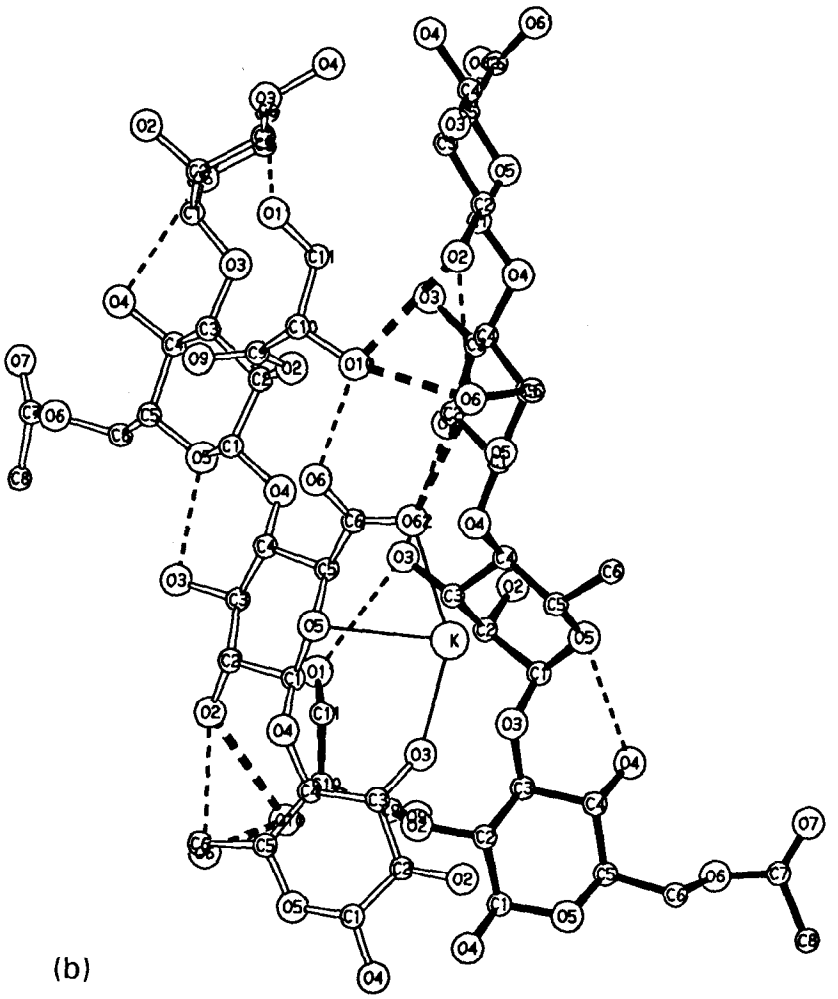

Fig. 7 (continued).

from an examination of the welan double-helix (Fig. 3) which underscores that the environment of the glucuronate residue is more crowded than the rest. On one side, atom O-2B at the bottom of the ring is hydrogen bonded to the acetyl group while atom O-3B at the top is involved in the cellulosic hydrogen bond. On the other side, atom O-62B of the carboxylate group at the top is an acceptor for hydrogen bonds with the main as well as side chain; and atom O-61B or O-62B serves as ligand to a calcium ion and/or forms hydrogen bond with a water molecule. Thus, it would seem that the large axial rise observed for the glucuronate residue is a major structural requirement for avoiding steric repulsion with one or more functional groups of the substituents.

The side-chain conformation angles (ϕ_5, ψ_5) in calcium welan are only (2°, 3°) away from the predicted values (column 3, Table IV). This remarkable agreement

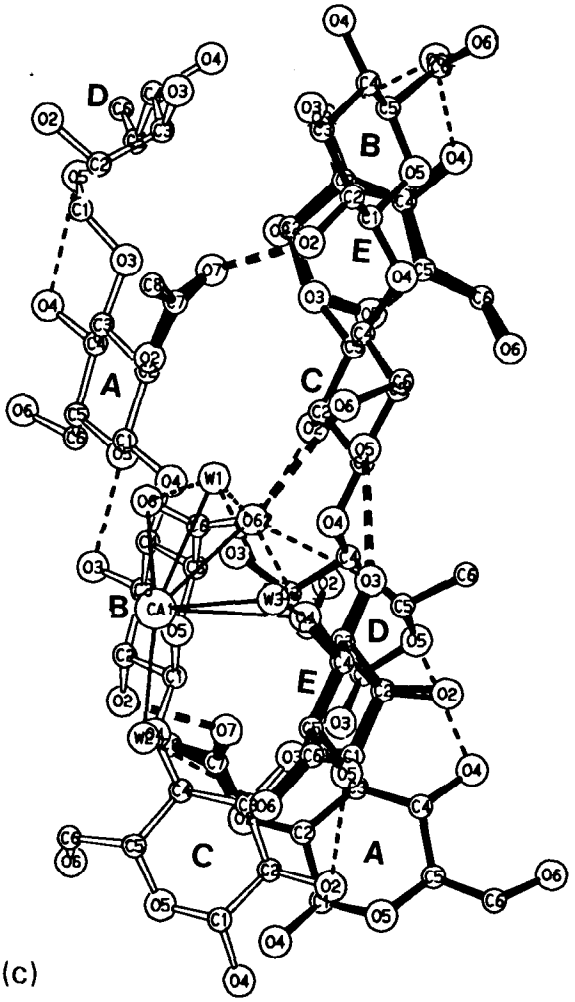

Fig. 7 (continued).

between theory and experiment suggests that molecular models, based on known parent structure, can be developed with confidence for related branched polymers as in the gellan family for which only meager X-ray data are available[14].

Hydrogen bonds.—Of the three intrachain hydrogen bonds O-3B · · · O-5A, O-2A · · · O-61B, and O-2B · · · O-6C in K^+ gellan, only the first is present in Ca^{2+} welan (Table V). It is interesting to note that the O-3B · · · O-5A distance is largest (2.92 Å) in gellan, intermediate (2.73 Å) in native gellan[24], and shortest (2.46 Å) in welan and this trend also has significant bearing on the extent of substitution on atom O-2A, the orientation of the carboxylate group and nature of the ionic surroundings in each case (Fig. 7). A K^+ ion is located on the surface of the double helix (Fig. 7a), close to the helix axis, between interstrand residues A and C and it makes contacts with both of them in gellan[15]; in contrast, the K^+ ion in

native gellan[24] is much closer to one chain, thereby making contacts only to its residues B and C (Fig. 7b). Thus, the ion is able to make contacts with both chains in gellan, but with one chain only in native gellan because of the glyceryl substitution[24]. The Ca^{2+} ion in welan, however, occurs outside the double helix, but makes close contact with residue B (Fig. 7c). The environment of residue A with its acetyl group, and that of the calcium and carboxylate group are such that residue B is compressed towards residue A. This leads to a decrease in the distance of O-3B · · · O-5A (2.46 Å). The second hydrogen bond O-2A · · · O-61B is not possible in native gellan or welan because of substitution. On the other hand, the third hydrogen bond O-2B · · · O-6C, present in gellan and native gellan, is absent in welan due to substantial movement of atom O-6C, as already inferred from the value of χ_3 in relation to gellan. In its place, a new interchain hydrogen bond O-2B · · · O-7A is formed. The intrachain hydrogen bonds O-4A · · · O-5D and O-3D · · · O-2C (second and third entries in Table V) are the same as in native gellan[24], but their distances (mainly dependent on ϕ_1 and ψ_4) 3.32 and 3.38 Å, respectively, are too long to be reckoned as hydrogen bonds in K^+ gellan.

Interactions between double helices.—The influence of substitution on the main chain is also seen on molecular packing. As the intermolecular separation increases from 9.1 Å in gellan[15], to 9.4 Å in native gellan[24], the number of main chain–main chain hydrogen bonds per repeating unit decreases from three in gellan to just one in native gellan; and at 12.0 Å apart, there is no direct involvement of the main chains alone in the association of the welan double helices. Instead there is one side chain–main chain or side chain–side chain hydrogen bond between the double helices (Table V). This implies that the aggregation of the welan double helices, particularly in solution, would be somewhat weaker than that in gellan.

DISCUSSION

The present crystal-structure analysis confirms the previous proposal[14] that welan can form a gellan-like, half-staggered, double helix in which the side chains do not disrupt, but rather stabilize, the ordered structure. Conformational differences noted in Table IV in relation to gellan are due primarily to the side chains and acetyl groups and perhaps to the type of cations used. By forming intrachain O-4E · · · O-62B and O-3E · · · O-62B hydrogen bonds, the side chains anchor the carboxylate groups in such a fashion that two double helices can associate through a calcium ion with or without a water molecule. The partial "physical screening" of the carboxylate groups by the side chains might explain why welan molecules would be ordered in aqueous solution, but would be random coils in a hydrogen bond breaking solvent like Me_2SO[13]. The removal of side chains would cause the carboxylate groups to be completely exposed to the surroundings as in gellan. Consequently, an order–disorder transition as a function of temperature could be followed in aqueous solutions for gellan, but not for welan[10].

The packing arrangement in the unit cell shows that welan double helices can associate in a parallel and two antiparallel modes either through calcium ions and water molecules or through side chains alone. For example, the carboxylate groups of double helices I and II (indicated by arrows in Fig. 6a) are not linked together by the calcium ion which is connected only to II. The double helices are, however, joined by side chain–side chain hydrogen bonds which are clearly seen above and below the arrows. For the parallel pair I and III, the carboxylate groups near the arrows (Fig. 6b) are oriented such that the distance between O-61B(I) and O-61B(III) is 4.6 Å. A calcium ion (Ca-1) located below both of them is close to the former, but its interaction with the latter is mediated via a water molecule. The double helices in this case are stabilized by $COO^- \cdots Ca^{2+} \cdots W \cdots COO^-$ interactions. On the other hand, the carboxylate groups of II and III face each other (Fig. 6c) such that the distance between atoms O-62B(II) and O-62B(III) is 5.6 Å; a calcium ion (Ca-2) between them leads to direct $COO^- \cdots Ca^{2+} \cdots COO^-$ interactions similar to those proposed in the calcium gellan model[25]. We suspect that the charge on Ca-1 is partially shielded by the three water molecules (W1, W2, and W3) surrounding it so that the total negative charge on three carboxylate groups is neutralized by the remaining net positive charge on the two calcium ions.

Previous studies have suggested that side chains might abolish the cation-induced aggregation process, perhaps by screening the carboxylate groups and making them unavailable for cation binding[10,14]. The results of this study demonstrate that side chains in welan fold back along the backbone, form hydrogen bonds with the main chain and thus stabilize the ordered structure. Specific features of the solid state structure such as the larger intermolecular separation of 12.0 Å rather than of the 9.1 Å in gellan, requirement of a water molecule to complete the $COO^- \cdots Ca^{2+} \cdots W \cdots COO^-$ crosslink between I and III, and complete absence of any direct Ca^{2+} involvement between I and II, however, suggest that welan double helices in solution would be limited to looser associations than those of gellan. Such aggregates could lead to "weak gel" formation in contrast to the strong gelling behavior of gellan in which calcium ions could mediate direct crosslinking of the carboxylate groups of double helices[25].

It is thus clear from the foregoing results that the welan double-helix is more stable than that of gellan. From the application of Smidsrød and Haug's treatment[26] to the data for intrinsic viscosity versus ionic strength, it was concluded that the stiffness of the welan chain is in the same range as that of DNA[11,12]. We might then expect that the molecular structure and organization within such a stiffened region would be most like the extended double helix we have elucidated in hydrated fibers. Stability of this type could explain why the ordered conformation of welan would remain unaltered in aqueous solution over a wide range of temperature[10–12]. If the peripheral side chain–side chain and side chain–main chain hydrogen-bonds are disturbed by using a solvent such as Me_2SO, the carboxylate groups would become exposed to the surroundings and welan would

undergo a rapid irreversible conformational transition to a disordered coil as reported by Hember et al[13].

The simultaneous occurrence of weak, medium, and strong intermolecular interactions in the crystal structure implies that each type might be responsible for certain useful rheological properties of welan. For example, the strong interactions might be relevant for concrete mix, while the medium and weak interactions for viscous solutions at low and high temperatures, respectively.

ACKNOWLEDGMENTS

This work was supported in part by the Industrial Consortium of the Whistler Center, Kelco, Division of Merck, the National Science Foundation (MCB-9219736) and the Purdue Research Foundation.

REFERENCES

1 P.-E. Jansson, B. Lindberg, G. Widmalm, and P.A. Sandford, *Carbohydr. Res.*, 139 (1985) 217–223.
2 M.A. O'Neill, R.R. Selvendran, V.J. Morris, and E.J. Eagles, *Carbohydr. Res.*, 147 (1986) 295–313.
3 P.-E. Jansson, B. Lindberg, and P.A. Sandford, *Carbohydr. Res.*, 124 (1983) 135–139.
4 J.D. Stankowski and S.G. Zeller, *Carbohydr. Res.*, 224 (1992) 337–341.
5 R. Moorhouse, in M. Yalpani (Ed.), *Industrial Polysaccharides: Genetic Engineering, Structure / Property Relations and Applications*, Elsevier, Amsterdam, 1987, pp 187–206.
6 A. Jeanes, C.A. Knutson, J.E. Pittsley, and P.R. Watson, *J. Appl. Polym. Sci.*, 9 (1965) 627–637.
7 A. Jeanes, *J. Polym. Sci.*, (1974) 209–227.
8 A. Darke, E.R. Morris, D.A. Rees, and E.J. Welsh, *Carbohydr. Res.*, 66 (1978) 133–144.
9 V. Crescenzi, M. Dentini, and I.C.M. Dea, *Carbohydr. Res.*, 160 (1987) 283–302.
10 V. Crescenzi, M. Dentini, T. Coviello, and R. Rizzo, *Carbohydr. Res.*, 149 (1986) 425–432.
11 S. Campana, C. Andrade, M. Milas, and M. Rinaudo, *Int. J. Biol. Macromol.*, 12 (1990) 379–384.
12 G. Robinson, C.E. Manning, and E.R. Morris, in E. Dickinson (Ed.), *Food Polymers, Gels and Colloids*, Royal Society of Chemistry Special Publication 82, 1991, pp 22–33.
13 M.W.N. Hember, R.K. Richardson, and E.R. Morris, *Carbohydr. Res.*, (accompanying paper H-2255).
14 E.J. Lee and R. Chandrasekaran, *Carbohydr. Res.*, 214 (1991) 11–24.
15 R. Chandrasekaran, L.C. Puigjaner, K.L. Joyce, and S. Arnott, *Carbohydr. Res.*, 181 (1988) 23–40.
16 L. Makowski, *J. Appl. Crystallogr.*, 11 (1978) 273–283.
17 R.D.B. Fraser, E. Suzuki, and T.P. MacRae, in I.H. Hall (Ed.), *Structure of Crystalline Polymers*, Elsevier, New York, 1984, pp 1–37.
18 R.P. Millane, and S. Arnott, *J. Macromol. Sci. Phys.*, 24 (1985) 193–227.
19 P.J.C. Smith, and S. Arnott, *Acta Crystallogr. Sect. A*, 34 (1978) 3–11.
20 *International Tables For X-Ray Crystallography*, Vol. IV, Kynoch Press, United Kingdom, 1974, pp 99–101.
21 S. Arnott, R. Chandrasekaran, A.W. Day, L.C. Puigjaner, and L.M. Watts, *J. Mol. Biol.*, 149 (1981) 489–505.
22 W.C. Hamilton, *Acta Crystallogr.*, 18 (1965) 502–510.
23 K.H. Gardner and J. Blackwell, *Biopolymers*, 13 (1974) 1975–2001.
24 R. Chandrasekaran, A. Radha, and V.G. Thailambal, *Carbohydr. Res.*, 224 (1992) 1–17.
25 R. Chandrasekaran, and V.G. Thailambal, *Carbohydr. Polym.*, 12 (1990) 431–442.
26 O. Smidsrød, and A. Haug, *Biopolymers*, 10 (1971) 1213–1227.